Modification of Hydroxyapatite Nanosurfaces for Enhanced Colloidal Stability and Improved Interfacial Adhesion in Nanocomposites

Hong Jae Lee, Hyung Woo Choi, Kyung Ja Kim, and Sang Cheon Lee*

Nanomaterials Application Division, Korea Institute of Ceramic Engineering and Technology, 233-5 Gasan-Dong, Guemcheon-Gu, Seoul 153-801, Korea

Received May 15, 2006. Revised Manuscript Received August 9, 2006

This work describes a rational approach of hydroxyapatite (HAp) nanosurface modification for graft polymerization of ϵ-caprolactone (CL). The ring-opening polymerization of CL on HAp surfaces was carried out using three types of HAp with different surface hydroxyl functionality: unmodified HAp (surface OH), HAp modified with L-lactic acid (secondary OH), and HAp modified with ethylene glycol (primary OH). The grafting efficiency and the amount of grafted poly(ϵ-caprolactone) (PCL) were dependent on the nature and steric environment of the hydroxyl groups on the HAp surfaces. Transmission electron microscopy measurements and time-dependent phase monitoring indicated that surface-modified HAp could be more uniformly dispersed in methylene chloride than unmodified HAp, and its colloidal stability increased dramatically as the amount of grafted PCL increased. The nanocomposites of PCL and PCL-grafted HAp showed enhanced tensile strength and toughness, compared with that of unmodified HAp and PCL. Increased interfacial interaction parameters ($B_{\sigma y}$) for the composite of PCL and PCL-grafted HAp strongly supported the enhanced mechanical strength of the nanocomposites. The use of HAp modified with a larger amount of PCL was found to be much more effective in improving mechanical properties of the nanocomposites.

Introduction

The use of hydroxyapatite (HAp) nanocrystals has caused an expanding interest in the fabrication of artificial bonelike ceramic/polymer composites due to its similarity to bone minerals in size, crystallinity, and morphology.[1−5] The nano-HAp not only plays a significant role in maintaining the mechanical properties of the natural bone but also offers a favorable environment for osteoconduction, protein adhesion, and osteoblast proliferation.[6] To produce the composites with bonelike properties, it is necessary to tailor the chemical nature of the HAp nanosurface. It is known that the strong interfacial adhesion between inorganic fillers and the organic polymer matrix is a key in generating the composites with good mechanical properties.[7−9] Thus, as an attempt to improve the interfacial adhesion, the surface of HAp nanocrystals has been modified with a diverse class of coupling agents and polymers through the chemical reaction with hydroxyl groups on the HAp surface.[10−21]

The colloidal stability of the nano-apatite in solutions as well as dispersibility in the nanocomposites is another important factor for fabrication of the nano-HAp containing polymer matrix.[20,22,23] Because the solution process is usually required to make the composites, obtaining the homogeneous and stable dispersion of nano-apatite in solutions is critical in producing the nanocomposites with the uniform structure and bulk properties.

Of a diverse class of composites, the combination of HAp and biodegradable polymers such as poly(L-lactide) and polycaprolactone is a choice of great importance due to their

* To whom correspondence should be addressed. Tel.: 82-2-3282-2469. Fax: 82-2-3282-7811. E-mail: sclee@kicet.re.kr.

(1) Zhang, W.; Liao, S. S.; Cui, F. Z. *Chem. Mater.* **2003**, *8*, 3221−3226.
(2) Song, J.; Malathong, V.; Bertozzi, C. R. *J. Am. Chem. Soc.* **2005**, *127*, 3366−3372.
(3) Song, J.; Saiz, E.; Bertozzi, C. R. *J. Am. Chem. Soc.* **2003**, *125*, 1236−1243.
(4) Hartgerink, J. D.; Beniash, E.; Stupp, S. I. *Science* **2001**, *294*, 1684−1688.
(5) Wei, G.; Ma, P. X. *Biomaterials* **2004**, *25*, 4749−4757.
(6) Murugan, R.; Ramakrishna, S. *Biomaterials* **2004**, *25*, 3829−3835.
(7) Xie, X. L.; Tang, C. Y.; Zhou, X. P.; Li, R. K. Y.; Yu, Z. Z.; Zhang, Q. X.; Mai, Y. W. *Chem. Mater.* **2004**, *16*, 133−138.
(8) Ji, X.; Hampsey, J. E.; Hu, Q.; He, J.; Yang, Z.; Lu, Y. *Chem. Mater.* **2003**, *15*, 3656−3662.
(9) Eitan, A.; Jiang, K.; Dukes, D.; Andrews, R.; Schadler, L. S. *Chem. Mater.* **2003**, *15*, 3198−3201.
(10) Murugan, R.; Ramakrishna, S. *Biomaterials* **2004**, *25*, 3073−3080.
(11) Liu, Q.; de Wijn, J. R.; van Blitterswijk, C. A. *J. Biomed. Mater. Res.* **1998**, *40*, 257−263.
(12) Liu, Q.; de Wijn, J. R.; van Blitterswijk, C. A. *J. Biomed. Mater. Res.* **1998**, *40*, 358−364.
(13) Liu, Q.; de Wijn, J. R.; van Blitterswijk, C. A. *J. Biomed. Mater. Res.* **1998**, *40*, 490−497.
(14) Liu, Q.; de Wijn, J. R.; van Blitterswijk, C. A. *Biomaterials* **1997**, *18*, 1263−1270.
(15) D′Andrea, S. C.; Fadeev, A. Y. *Langmuir* **2003**, *19*, 7904−7910.
(16) Barralet, J. E.; Tremayne, M.; Lilley, K. J.; Gbureck, U. *Chem. Mater.* **2005**, *17*, 1313−1319.
(17) Tanaka, H.; Futaoka, M.; Hino, R.; Kandori, K.; Ishikawa, T. *J. Colloid Interface Sci.* **2005**, *283*, 609−612.
(18) Tanaka, H.; Futaoka, M.; Hino, R. *J. Colloid Interface Sci.* **2004**, *269*, 358−363.
(19) Borum-Nicholas, L.; Wilson, O. C., Jr. *Biomaterials* **2003**, *24*, 3671−3679.
(20) Borum, L.; Wilson, O. C., Jr. *Biomaterials* **2003**, *24*, 3681−3688.
(21) Liu, Q.; de Wijn, J. R.; de Groot, K.; van Blitterswijk, C. A. *Biomaterials* **1998**, *19*, 1067−1072.
(22) Hong, J.; Qiu, X.; Sun, J.; Deng, M.; Chen, X.; Jing, X. *Polymer* **2004**, *45*, 6699−6706.
(23) Hong, J.; Zhang, P.; He, C.; Qiu, X.; Liu, A.; Chen, L.; Chen, X.; Jing, X. *Biomaterials* **2005**, *26*, 6296−6304.

10.1021/cm061139x CCC: $33.50
Published on Web 09/13/2006

superiority in osteoconduction and sustained biodegradability.[24,25] To improve the interfacial adhesion in these composites, the HAp surfaces can be modified with the appropriate organic polymers using the surface hydroxyl groups. However, the direct use of surface hydroxyl groups was found not to be a good choice for the effective surface modification due to their limited reactivity. Recently, it was reported that the hydroxyl groups on HAp surfaces were not effective for initiating graft polymerization of L-lactide, and the maximum grafting amount of the polymer was as low as 6 wt %.[22,23] For this reason, the reactivity tuning of hydroxyl groups on HAp is an important subject to offer effective modification methods of HAp nanosurfaces.

To date, a systematic study to control the reactivity of surface hydroxyl groups of HAp nano-apatites has never been reported. This approach can generate the well-defined polymer structure on HAp nanosurfaces by controlling the grafting efficiency. Thus, surface engineering of HAp nano-apatites with controllable reactivity may play a significant role in producing property-adjustable HAp/polymer nanocomposites.

The aim of this study is to provide a systematic method of HAp nanosurface modification for graft polymerization of ϵ-caprolactone (CL). We are interested in knowing whether the presence of surface hydroxyl functionality with different nucleophilicities and the steric environment determines the anchoring efficiency of poly(ϵ-caprolactone) (PCL) onto HAp nanosurfaces. The enhanced colloidal stability of PCL-grafted HAp in organic solutions was described. Besides, the significant effect of the nanosurface modification on interfacial adhesion between inorganic HAp and the organic PCL matrix in the composites was described on the basis of interfacial interaction parameters. The reinforcing and toughening effectiveness of PCL-grafted HAp nanocrystals for nanocomposites was also discussed.

Experimental Section

Materials. Calcium hydroxide ($Ca(OH)_2$), phosphoric acid (H_3PO_4), L-lactic acid (2-hydroxypropionic acid), hexamethylene diisocyante (HMDI), dibutyltindilaurate, stannous octoate ($Sn(Oct)_2$), ethylene glycol (EG), and PCL (M_n = 80 000 g/mol) were purchased from Aldrich Co. (Milwaukee, WI) and used without further purification. CL was dried over calcium hydride and vacuum distilled. Tetrahydrofuran (THF) and toluene were distilled from Na/benzophenone under N_2, prior to use. *N*,*N*-Dimethylformamide (DMF) was vacuum distilled over anhydrous magnesium sulfate. The water was purified by distillation, deionization, and reverse osmosis (Milli-Q Plus) and used in the synthesis of HAp nanocrystals. All other reagents and chemicals were of the analytical grade.

Synthesis of HAp Nanocrystals. The HAp nanocrystals were prepared by a chemical precipitation and hydrothermal technique according to the modified literature procedure.[22] To a vigorously stirred aqueous solution of $Ca(OH)_2$ (0.25 M, 625 mL) was added an aqueous solution of H_3PO_4 (0.3 M, 300 mL) dropwise at a rate of 1 mL/min at 60 °C. After completion of H_3PO_4 addition, the pH of the suspension was adjusted to pH 7.0. After aging, HAp nanocrystals were purified and collected by repeated washing with distilled water and centrifugation at 2500 rpm for 20 min (×5). The final product, HAp nanocrystals, was obtained by freeze-drying.

Surface Modification of HAp with L-Lactic Acid (L-HAp). To a stirred suspension of HAp (3 g) in THF (21 mL) was added L-lactic acid (1.5 g, 0.017 mol). The reaction mixture was heated to 60 °C and kept there for 30 min. About 10 mL of THF was distilled off using a Dean−Stark apparatus, and dry toluene (40 mL) was added in the reaction flask. The reaction temperature was then elevated at 150 °C, and the reaction was maintained for 10 h. The water formed during the reaction was removed by azeotropic distillation with toluene. HAp modified with L-lactic acid (L-HAp) was purified and isolated by repeated washing with methylene chloride and centrifugation at 2500 rpm for 20 min (×5). The purified L-HAp was dried at 60 °C in vacuo for 24 h.

Surface Modification of HAp with EG (E-HAp). To a stirred suspension of HAp nanocrystals (3 g) in dry DMF (45 mL) were added HMDI (1.5 mL, 8.92 mmol) and dibutyltindilaurate (0.045 g, 0.07 mmol). The reaction was maintained at 50 °C under nitrogen for 8 h. A solution of EG (5.86 g, 0.094 mol) in DMF (5.86 mL) was added to the reaction mixture, and the mixture was stirred overnight at 60 °C. After the reaction, EG-grafted HAp (E-HAp) was purified and collected by repeated washing with methylene chloride and centrifugation at 2500 rpm for 20 min (×5). The isolated E-HAp was dried at 60 °C in vacuo for 24 h.

Graft Polymerization of CL on HAp Nanocrystals. The grafting reaction of PCL on HAp was performed using three classes of HAp (HAp, L-HAp, and E-HAp) with surface hydroxyl groups of different nucleophilicities and steric environments. As a typical process for PCL grafting on HAp, C-HAp obtained from unmodified HAp nanocrystals was prepared by the following procedure: A suspension of HAp (3 g) in dry toluene (50 mL) was heated at reflux using a Dean−Stark apparatus. Approximately 10 mL of toluene was evaporated, and the Dean−Stark apparatus was replaced by a condenser. At room temperature, CL (3 g, 26.28 mmol) and $Sn(Oct)_2$ (0.045 g) were added under nitrogen. The temperature was then raised to 130 °C. The reaction was maintained for 25 h. Samples were collected at a predetermined time to evaluate the time-dependent grafting amount of PCL onto HAp nanosurfaces. The mixture was diluted with methylene chloride, and the C-HAp was separated by a repeated washing−centrifugation cycle (×5) at 2500 rpm for 20 min. Other PCL-grafted HAp, LC-HAp and EC-HAp, which were obtained using L-HAp and E-HAp, were synthesized in an identical manner.

Solid-State ^{1}H Cross-Polarization Magic-Angle-Spinning (CP/MAS) NMR Analysis. The solid-state ^{1}H CP/MAS NMR spectra were recorded at 400 MHz on a Varian INOVA400 NMR spectrometer (Palo Alto, CA) with a sample spinning rate of 5 kHz at 25 °C. CP spectra were acquired with a delay time of 2.0 s, acquisition time of 3.7 s, and number of transients of 16.

Inductively Coupled Plasma Mass Spectroscopy (ICP-MS). ICP-MS was used for compositional analysis of HAp nanocrystals. ICP-MS analysis was carried out on a Perkin-Elmer Sciex Elan 6100 instrument (Wellesley, MA) using an argon plasma flame and dual detector mode. Standards for linear regression curves for Ca and P (0.1−10 ppm) were made by appropriate dilution of 1000 ppm standards. Samples (100 mg) were dissolved in a few drops HCl (100 mL) and diluted with doubly distilled water to obtain Ca and P concentrations within the range of the standards.

Brunauer−Emmett−Teller (BET) Analysis. The specific surface area of HAp nanocrystals was determined by BET nitrogen gas adsorption using a NOVA 4000e (Quantachrome Instruments, Boynton Beach, FL) surface area and pore size analyzer. Approximately 100 mg samples were placed into the sample cell,

(24) Boduch-Lee, K. A.; Chapman, T.; Petricca, S. E.; Marra, K. G.; Kumta, P. *Macromolecules* **2004**, *37*, 8959−8966.
(25) Deng, X.; Hao, J.; Wang, C. *Biomaterials* **2001**, *22*, 2867−2873.

Scheme 1. Reaction Routes for Graft Polymerization of CL on HAp Nanosurfaces

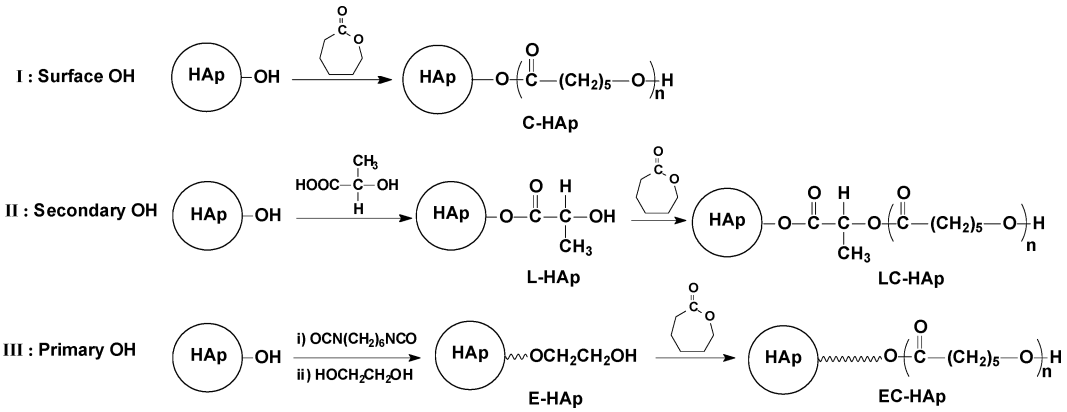

weighed, and outgassed under vacuum at a temperature of 120 °C for 1 h prior to sample measurement. Duplicate measurements were taken, and the mean specific surface area was calculated.

Thermal Gravimetric Analysis (TGA). The amount of the surface-grafted polymer on HAp nanocrystals was determined by TGA using a Mettler Toledo TGA/SDTA 851^e (Columbus, OH). TGA measurements were performed from room temperature to 800 °C at a rate of 5 °C/min. Nongrafted HAp and grafted HAp nanocrystals were used for TGA analysis. The amount of surface-grafted polymers was determined as a weight loss percentage during heating.

Fourier Transform Infrared (FT-IR) Spectroscopy. To prove the grafting of PCL on HAp nanocrystals, FT-IR spectra were recorded on a FT/IR-460 PLUS spectrometer (JASCO, Tokyo, Japan) in the range between 4000 and 650 cm^{-1}, with a resolution of 2 cm^{-1} and 64 scans. Both HAp and modified HAp nanocrystals were directly used for FT-IR measurements. The FT-IR spectra of the PCL homopolymer and nongrafted HAp were also obtained as controls to confirm the surface grafting of PCL on HAp nanocrystals.

Powder X-ray Diffraction (XRD). XRD measurements were performed with a Rigaku D/max-RB apparatus (Tokyo, Japan) powder diffractometer and image-plate photography using graphite-monochromatized Cu Kα radiation (λ = 1.542 Å). Data were collected from 10 to 60° with a step size of 0.05° and step time of 5 s.

Transmission Electron Microscopy (TEM). TEM was performed on a JEOL JEM-2000EX (Tokyo, Japan), operating at an acceleration voltage of 200 kV. To observe the size and shape of unmodified HAp and modified HAp nanocrystals and to estimate the dispersion state in methylene chloride, a drop of the sample solution in methylene chloride (concentration = 1 g/L) was placed onto a 200-mesh copper grid coated with carbon. The samples were air-dried before measurement.

Mechanical Testing. HAp, C-HAp, and EC-HAp were dispersed separately in methylene chloride, and PCL was added to each suspension to make the solution mixture. Each solution was poured into an excess of *n*-hexane to precipitate the HAp/PCL, C-HAp/PCL, and EC-HAp/PCL nanocomposites, respectively. The composites were dried in vacuo at room temperature for 24 h. For preparing specimens for tensile testing, pure PCL and the nanocomposites of HAp (10 wt %)/PCL, C-HAp (10 wt %)/PCL, and EC-HAp (10 wt %)/PCL were compressed by hot press molding at 100 °C and 15 MPa. The sample specimens with the dimension of 35 × 5 × 0.5 mm^3 were cut by a dog-bone shaped die. The tensile test was performed using a computer controlled mechanical Universal testing machine LLOYD LR50K (Fareham, U.K.) at a stretching rate of 20 mm/min and cross-head speed of 20 mm/min.

Results and Discussion

Synthesis and Characterization of HAp Nanocrystals. The precipitation reaction for HAp nanocrystals was carried out following an idealized stoichiometric equation as described below:

$$6H_3PO_4 + 10Ca(OH)_2 \rightarrow Ca_{10}(PO_4)_6(OH)_2(HAp) + 18H_2O$$

The crystalline structure of HAp nanocrystals identified by XRD belonged to the hexagonal crystal class with the space group; a = 94.2 nm and c = 68.8 nm. The specific surface area of HAp nanocrystals (N_2, BET) was found to be 70 m^2/g, which was close to the literature value.[18] The Ca/P molar ratio of HAp nanocrystals was 1.59, reflecting that the synthesized HAp is Ca^{2+}-deficient. TEM experiments showed that the HAp particles were acicular crystals, and the mean size was 120 nm in length and 20 nm in width.

Modification of HAp Nanosurfaces and Subsequent Graft Polymerization of CL. The graft polymerization of CL onto HAp nanosurfaces was carried out by thermal ring-opening polymerization of CL in the presence of HAp with surface hydroxyl functionality. For the systematic study of graft polymerization, the grafting reaction was performed using three different schemes as shown in Scheme 1. In reaction class I, the surface hydroxyl groups on HAp were directly used for initiating graft polymerization of CL. In reaction class II, L-lactic acid was allowed to react with surface hydroxyl groups to form secondary alcohol via lactate formation on HAp, and HAp modified with L-lactic acid was used for subsequent ring-opening polymerization of CL. For reaction class III, surface hydroxyl groups were first reacted with HMDI and further with EG in a one-pot reaction, and the chemical anchoring of PCL on HMDI-EG-modified HAp was performed to produce PCL-grafted HAp. Modified HAp in each reaction class was denoted as C-HAp, LC-HAp, and EC-HAp, respectively. We started the grafting reaction on the assumption that the steric environment and nucleophilicity of the hydroxyl groups may determine the efficiency of graft polymerization of CL on HAp nanosurfaces.

The reactivity control of hydroxyl groups on HAp surfaces is the first step for graft polymerization of CL. The HAp was modified by the reaction with L-lactic acid or EG via a HMDI-mediated coupling reaction. The modification of

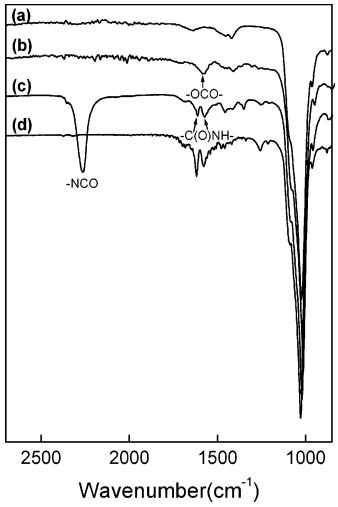

Figure 1. FT-IR spectra of (a) unmodified HAp, (b) L-HAP, (c) HAp-HMDI, and (d) E-HAp.

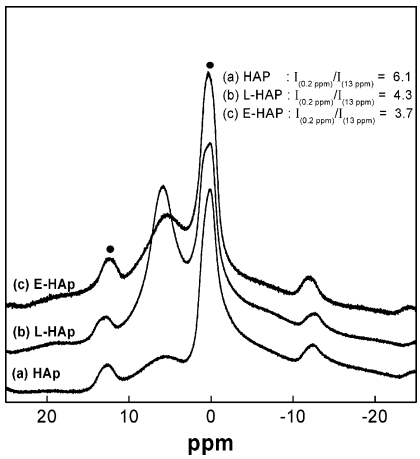

Figure 2. ^{1}H CP/MAS NMR spectra of HAp, C-HAp, and E-HAp.

L-HAp and E-HAp was confirmed by IR spectra in Figure 1. Compared with unmodified HAp in Figure 1a, L-HAp in Figure 1b shows the new vibrational bands at 1575 cm^{-1} originated from the −OCO− vibration, indicating the lactate formation on the HAp nanosurface. For E-HAp, the identification of −NHCO− linkages between the HAp surface and HMDI is critical because it may guarantee the chemical anchoring of PCL, which will be polymerized afterward. The IR spectrum of E-HAp in Figure 1c obviously exhibits the presence of −NHCO− at 1613 and 1580 cm^{-1} and free isocyanate bands at 2255 cm^{-1}. This indicates that the isocyanate at the one end of HMDI was coupled to HAp surfaces via chemical bonding, and the isocyanate at the other end was still active for the reaction with EG. After reaction of HAp-HMDI with EG, isocyanate bands completely disappear as shown in Figure 1d, reflecting the introduction of primary OH on HAp nanosurfaces.

A quantitative analysis for modification was carried out using ^{1}H NMR CP/MAS spectroscopy. Figure 2 shows the solid-state ^{1}H NMR CP/MAS spectra of HAp, L-HAp, and E-HAp. As reported in the previous reports, the structural hydroxyl groups of HAp including surface and bulk hydroxyl groups resonate at 0.2 ppm.[26] The chemical shifts at around

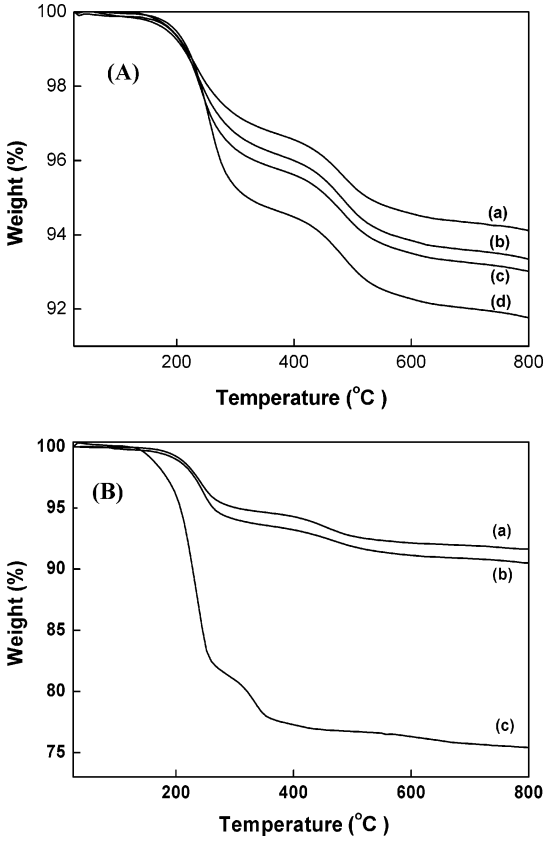

Figure 3. (A) TGA curves of C-HAp prepared at different reaction times: (a) 1 h, (b) 3 h, (c) 15 h, and (d) 25 h. (B) TGA curves of (a) C-HAp, (b) LC-HAp, and (c) EC-HAp prepared at a reaction time of 25 h.

5.0 ppm are ascribed to the surface-adsorbed water or the surface-linked organic compounds. The downfield chemical shift at 13.0 ppm was known to be from the hydrogen-bonding protons in the bulk structure of HAp. This characteristic resonance at 13.0 ppm can be used as the reference peak for the reaction with surface hydroxyl groups because the modification reaction at the surface of HAp does not affect its peak intensity.[21,26] On the basis of the calculation of the peak intensity at 0.2 ppm using the peaks at 13.0 ppm as a reference, it could be found that the peak intensity at 0.2 ppm decreased by 29 and 42% for L-HAp and E-HAp, respectively. This strongly supports that the hydroxyl groups of 29 and 42% on HAp surfaces were converted to surface hydroxyl functionalities with different reactivity.

The graft polymerization of CL was performed using three types of HAp in the presence of $Sn(Oct)_2$ as a catalyst. Figure 3A shows TGA curves of HAp prepared at different reaction times. The plots provide the information on the time-dependent grafting amount of PCL on HAp. Inorganic HAp nanocrystals fully dried at 150 °C for 48 h underwent the weight loss less than 1 wt % up to 800 °C, and thus the weight loss in Figure 3 is exclusively ascribed to the organic substances, the grafted PCL. The percent grafting of PCL on HAp nanosurfaces and grafting efficiency were determined by eqs 1 and 2, respectively.

(26) Yesinowski, J. P.; Eckert, H. *J. Am. Chem. Soc.* **1987**, *109*, 6274−6282.

$$\text{percentage of grafting (\%)} = \frac{\text{grafted PCL on HAp (g)}}{\text{PCL-grafted HAp (g)}} \times 100 \quad (1)$$

$$\text{grafting efficiency (\%)} = \frac{\text{grafted PCL on HAp (g)}}{\text{CL used (g)}} \times 100 \quad (2)$$

The grafted PCL (g) on HAp was measured by TGA, and CL is the feed amount for graft polymerization.

The PCL grafting amount at a reaction time of 1 h was 6.0 wt % and gradually increased as the reaction time increased. The maximum grafting amount of PCL on HAp was obtained at a reaction time of 25 h, and the 8.4 wt % PCL was grafted on HAp surfaces. Further grafting reaction over 25 h did not contribute to the increase of the PCL grafting amount (data not shown). Figure 3B shows the TGA curves of PCL-grafted HAp prepared through three different reaction schemes at a reaction time of 25 h. As listed in Table 1, the PCL grafting amount on LC-HAp (9.5 wt %) is a little higher than that of C-HAp (8.4 wt %). The surface hydroxyl groups on HAp surfaces have intrinsic steric hindrance for attacking carbonyl carbons of CL. Thus, it seems that the modification of surface hydroxyl groups by lactate led to the slight increase in grafting amount of PCL, but not to a great extent. Considering modification of 29% of the surface hydroxyl groups, it is likely that the secondary alcohol with a short chain on L-HAp could not overcome the steric hindrance for CL polymerization. On the other hand, it is of great interest to note that EC-HAp prepared by E-HAp has the PCL grafting amount and grafting efficiency of as much as 24.6 wt % and 47%, respectively. This enhanced grafting efficiency of E-HAp for PCL can be explained by the synergistic effect from following two possible reasons: One is the nucelophilicity of hydroxyl groups on HAp surfaces. The hydroxyl groups on E-HAp are primary OH, and thus they can initiate the polymerization of CL more easily than surface hydroxyl groups on unmodified HAp and secondary OH on L-HAp. The other is the steric environment of hydroxyl groups. The hydroxyl groups of E-HAp are linked to the HAp surface via a relatively long chain spacer (**HAp**-$OCONH(CH_2)_6NHOCOCH_2CH_2$-***OH***). For this reason, the steric hindrance of the hydroxyl group seems to be very low, and it may have more accessibility to CL for graft polymerization. Thus, it can be suggested that the key factor for effective graft polymerization of CL is ascribed not only to the nucleophilicty but also to the steric environment of the surface hydroxyl groups. The dependency of reaction time and the reaction class on the PCL grafting amount was summarized in Table 1. Figure 4 shows IR spectra of pure PCL, HAp, and three PCL-grafted HAp, C-HAp, LC-HAP, and EC-HAp, respectively. The C═O stretching at 1734 cm^{-1} was observed for all PCL-grafted HAp. As expected, the intensity of C═O is proportional to the grafted PCL amount and increased in an order of C-HAp, LC-HAp, and EC-HAp.

The XRD patterns of unmodified HAp and PCL-grafted HAp are shown in Figure 5. Surface modification should be an event occurring only at the HAp nanosurfaces. If the chemical reaction alters the state of the bulk properties such as crystallinity and the crystalline phase, the resulting HAp loses its intrinsic properties.[18] Thus, confirmation of the selective reaction on the HAp surfaces and the maintenance of crystalline properties of HAp is important. The diffracted peaks of unmodified HAp are consistent with those of the pure HAp phase. The characteristic peaks at 2θ regions of 26°, 29°, 32−34°, 40°, and 46−54° indicated the crystalline nature of HAp nanocrystals. As shown in Figure 5, the grafting reaction did not induce any change in crystalline phase of HAp nanocrystals. Besides, any secondary phases were not formed due to the chemical reaction. This supports the selective chemical modification and graft polymerization on the nanosurfaces of HAp.

Table 1. Dependency of the PCL Grafting Amount and the Grafting Efficiency on Reaction Time and Reaction Class[a]

percent grafting of PCL on HAp nanocrystals[b] and grafting efficiency[c] (%)						
dependency on reaction time[d]				dependency on reaction class		
1 h	3 h	15 h	25 h	I	II	III
6.0 (11)	6.8 (12)	7.1 (14)	8.4 (16)	8.4 (16)	9.5 (20)	24.6 (47)

[a] All samples synthesized for 25 h were used for TGA. [b] Percent grafting was calculated using eq 1. [c] Grafting efficiency was calculated using eq 2 and was listed in the parenthesis. [d] Time-dependent percent grafting of PCL was estimated for C-HAp by TGA.

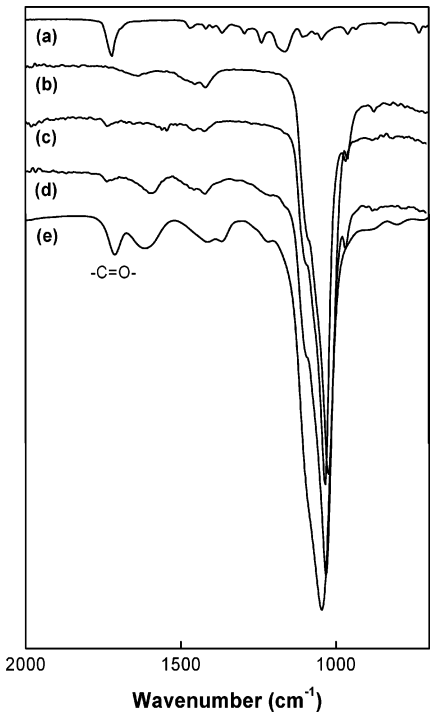

Figure 4. FT-IR spectra of (a) pure PCL, (b) unmodified HAp, (c) C-HAp, (d) LC-HAP, and (e) EC-HAp.

Colloidal Stability and Dispersivity of PCL-Grafted HAp nanocrystals. The HAp nano-apatite tends to aggregate to form microscale clusters due to interparticle van der Waals interaction as well as the hydrogen bonding between surface hydroxyl groups.[20,27] For example, when HAp nanocrystals are allowed to disperse in solvents, they do not maintain the colloidal stability and tend to precipitate within 1 min. Most methods for preparation of the organic−inorganic nanocomposites are based on the solution process. For this reason, the main requirement to obtain the homo-

(27) Liu, Y.; Nancollas, G. H. *J. Phys. Chem. B* **1997**, *101*, 3464−3468.

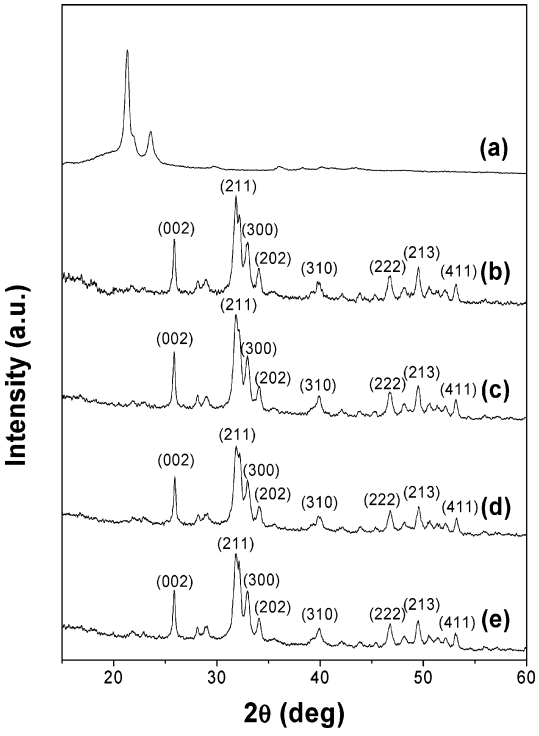

Figure 5. XRD patterns of (a) PCL, (b) unmodified HAp, (c) C-HAp, (d) LC-HAp, and (e) EC-HAp.

geneous bulk properties is the uniform dispersion of inorganic fillers at the nano-level in the polymer matrix. Thus, to date, the improvement of the dispersion properties and the colloidal stability of HAp particles in solutions is one of the important issues.[19,20] Figure 6 shows the TEM images of unmodified HAp and three PCL grafted HAp nanocrystals (C-HAp, LC-HAp, and EC-HAp) of which TEM samples were prepared from the solutions of methylene chloride, a good solvent for PCL. It is noteworthy that the PCL-grafted HAp crystals showed a much improved dispersion property, compared with unmodified HAp. Besides, the dispersion state improved as the grafting amount of PCL increased. EC-HAp with 24.6 wt % of grafted PCL exhibits the most excellent dispersibility in methylene chloride. Monitoring of time-dependent colloidal stability of unmodified HAp and PCL-grafted HAp in methylene chloride is illustrated in Figure 7. The colloidal stability dramatically increased as the amount of grafted PCL increased. Pure HAp nano-apatite did not maintain stability and precipitated in methylene chloride within 3 min. In the case of C-HAp with a relatively low PCL content, the colloid stability increased slightly.

This indicates that the lower level of PCL grafting could not overcome the interparticle interaction and the high density of HAp (3.2 g/mL).[28] Interestingly, EC-HAp with the highest grafting amount of PCL showed the excellent colloidal stability. This tendency is in good accordance with the dispersion state of nanocrystals in the TEM results (Figure 6).

HAp/PCL Nanocomposites. Once it was confirmed that the effective PCL grafting on HAp nanocrystal greatly enhanced the colloidal stability and dispersion property, the next question is whether the use of PCL-grafted HAp in making HAp/PCL nanocomposites can play a role in improving the mechanical properties of the composites. For preparation of HAp/PCL nanocomposites with enhanced mechanical properties and homogeneous bulk properties, the good dispersion of HAp nanocrystals at the nano-level in the polymer matrix is important. When HAp with a fair amount of grafted-PCL, that is, EC-HAp, is mixed with PCL in a solution, uniform dispersion of HAp in the polymer matrix is expected due to the improved dispersivity of EC-HAp in an organic phase as shown in Figures 6 and 7. Thus, the nanocomposites produced via a solution process may contain uniformly distributed HAp single nanocrystals.

Surface-modified HAp may lead to the improved interfacial adhesion between two phases, the organic PCL matrix and inorganic HAp nanocrystals, because the chemically grafted PCL on HAp can fuse into and entangle with the PCL chains in the polymer matrix. Figure 8 shows the stress−strain profile of pure PCL, HAp/PCL, C-HAp/PCL, and EC-HAp/PCL, at 25 °C in dry conditions, respectively. The mechanical properties are summarized in Table 2. Pure PCL undergoes the typical stress−stain behavior of semicrystalline elastic polymers, yielding, rubbery plateau, and fracture. For the HAp/PCL composite, it is noteworthy that the addition of HAp into the PCL matrix increased the tensile modulus and strength respectively from 2.6 and 20.3 MPa to 3.2 and 22.1 MPa, but the toughening behavior of PCL itself was decreased. This behavior can be correlated with the dispersion state of HAp prepared from the organic solution (Figure 7). The intra-structural environment of the composites may have a defect due to the aggregated HAp in the PCL matrix. Thus, it is likely that the stress concentration around the region of inorganic HAp aggregates resulted in the early failure and fracture. On the other hand, the C-HAp/PCL composites showed enhanced tensile modulus and strength and toughness, compared with HAp/PCL. This can be ascribed to the improved interfacial adhesion between inorganic HAp and the PCL matrix. It is of great interest to note that the EC-HAp/PCL containing HAp with 24.6 wt % of grafted PCL exhibited the most significant improvement not only in the tensile modulus and strength but also in toughness. The tensile modulus and strength of EC-HAp/PCL relative to the HAp/PCL composite increased by 72 and 28%, respectively. The excellent dispersibility of EC-HAp as well as the strong adhesion at the interface supports this improved mechanical property. The data in this work suggests that the PCL-grafted HAp is suitable for both reinforcing and toughening of the apatite-containing PCL composites. On the basis of the effects of C-HAp and EC-HAp on the mechanical properties of the composites, it can be suggested that the reactivity tuning of HAp surface hydroxyl groups proposed in this study resulted in the production of the property-adjustable nanocomposites by controlling the grafted PCL amounts on HAp surfaces.

In previous reports, it was known that the tensile strength of the composites was affected by the interfacial adhesion.[29,30] Turcsanyi et al. demonstrated the relationship between tensile

(28) Ciapetti, G.; Ambrosio, L.; Savarino, L.; Granchi, D.; Cenni, E.; Baldini, N.; Pagani, S.; Guizzardi, S.; Causa, F.; Giunti, A. *Biomaterials* **2003**, *24*, 3815−3824.
(29) Turcsanyi, B.; Pukanszky, B.; Tudos, F. *J. Mater. Sci. Lett.* **1988**, *7*, 160−162.

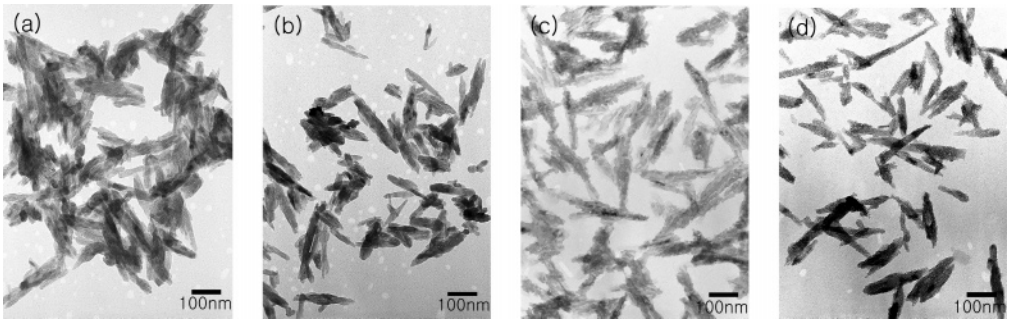

Figure 6. TEM images of (a) unmodified HAp, (b) C-HAp, (c) LC-HAp, and (d) EC-HAp.

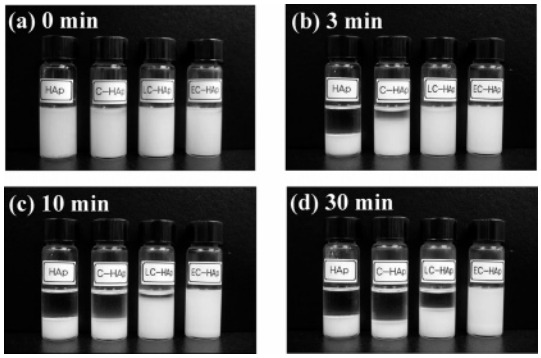

Figure 7. Monitoring of time-dependent colloidal stability of HAp, C-HAp, LC-HAp, and EC-HAp in methylene chloride (from left to right): (a) 0 min, (b) 3 min, (c) 10 min, and (d) 30 min.

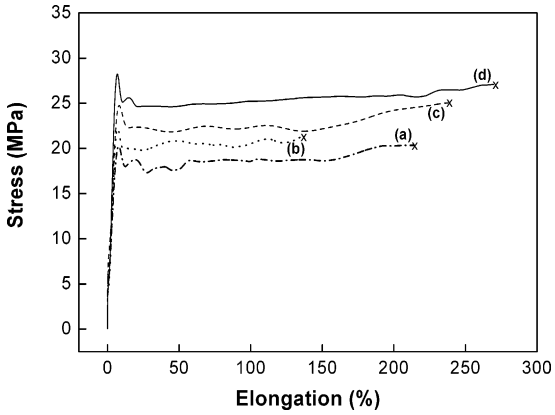

Figure 8. Stress−strain curves of (a) pure PCL, (b) the HAp (10 wt %)/PCL nanocomposite, (c) the C-HAp (10 wt %)/PCL nanocomposite, and (d) the EC-HAp (10 wt %)/PCL nanocomposite.

Table 2. Mechanical Properties of PCL, HAp/PCL, C-HAp/PCL, and EC-HAp/PCL

specimen	tensile modulus (MPa)	tensile strength (MPa)	ultimate longation at break (%)	interfacial interaction parameter ($B_{\sigma y}$)
pure PCL	2.6	20.3	213.7	
HAP (10 wt %)/PCL	3.2	22.1	136.5	5.77
C-HAP (10 wt %)/PCL	3.6	25.0	237.9	7.96
EC-HAP (10 wt %)/PCL	5.5	28.2	269.6	9.54

strength and interfacial interaction on the basis of the following equation:[29]

$$\sigma_y = \sigma_{ym}\frac{1-\phi_f}{1+2.5\phi_f}\exp(B_{\sigma y}\phi_f) \qquad (3)$$

where σ_y and σ_{ym} represent yield stresses of the composite and the polymer matrix, respectively. ϕ_f is the volume fraction of the filler particles, and $B_{\sigma y}$ is an interfacial interaction parameter. In general, the larger $B_{\sigma y}$ results in the stronger adhesion in the interface. When eq 3 was used, $B_{\sigma y}$ was calculated for HAp/PCL, C-HAp/PCL, and EC-HAp/PCL composites. As listed in Table 2, $B_{\sigma y}$ is 5.77 for the HAp/PCL composite, whereas $B_{\sigma y}$ is found to increase to 7.96 and 9.54 for C-HAp and EC-HAp/PCL, respectively. This indicates that the PCL grafting on HAp nanosurfaces is effective in improving the interfacial adhesion between HAp nanocrystals and the PCL matrix. Besides, the interfacial interaction increased depending on the amount of grafted PCL. Using a composite of surface modified glass beads and poly(phenylene oxide), Xie et al. demonstrated that the modified surface contributed to the improvement of the tensile strength of the composites.[7] They also described a good quantitative relation between the tensile strength and the interfacial adhesion. The interfacial adhesion parameter is known to be a sensitive parameter, and thus the increase of about 10% in $B_{\sigma y}$ led to the substantial improvement of the tensile strength of the composites.[7] In our system, the use of EC-HAp resulted in the 65% increase of the $B_{\sigma y}$ parameter, and this increase was reflected in the about 30% increase of the tensile strength. For EC-HAp/PCL, the excellent adhesion in the interface possibly originates from the penetration of grafted PCL on HAp surfaces into the PCL matrix. More specifically, PCL chemically linked to the HAp surface can participate in the crystallization of the PCL matrix during the melt processing for nanocomposites. Thus, it can be suggested that the PCL anchoring on the HAp nanosurface and the grafted PCL amount are key factors for the strong adhesion between the PCL matrix and the HAp nanocrystals. For nanocomposites of PCL-grafted HAp and PCL featuring the strong adhesion between organic and inorganic phases, the PCL chains first orientate and elongate rather than the initial dewetting and cavitation at the interface of inorganic HAp filler and the PCL matrix. For this reason, the nanocomposite prepared in our approach exhibits improved toughness, compared with the composites from unmodified HAp and PCL. On the basis of the preliminary study, we confirmed that PCL-grafted HAp showing the good dispersibility in solutions could serve as an excellent adhesion enhancer between organic PCL phases and inorganic HAp phases, thereby contributing to the improvement of the mechanical properties of nanocomposites.

(30) Pukanszky, B. Particulate-filled polypropylene: structure and properties. In *Polypropylene-structure, blends and composites*; Karger-Krocsis, J., Ed.; Chapman & Hall Press: New York, 1995; Vol. 3.

The originality of this work is the systematic modulation of reactivity of HAp nanosurfaces for controlled grafting polymerization. This type of controlled reactivity and subsequent polymerization has never been reported in the growing field of organic−inorganic nanocompsoites. This adjusted reactivity of HAp surfaces has a significant meaning because it determines the grafting efficiency of polymers and finally gives a big effect on enhanced colloidal stability of HAp nanocrystals in solutions. The better dispersion and colloidal stability of modified HAp that could be achieved through the approach of this work was directly related to the improved mechanical properties of the organic−inorganic nanocomposites. Our preliminary work for in vitro evaluation of protein adsorption and cell attachment/proliferation on composites showed that the chemically grafted HAp nanocrystals offered the favorable environments for bone regeneration due to the excellent disperion at the nano-level in the composites. The details on biological evaluation of the composites will be reported elsewhere.

Conclusions

We described the systematic approach to control the reactivity of surface hydroxyl groups on HAp nanocrystals and subsequent graft polymerization of CL. The choice of hydroxyl groups with a high degree of nucleophilicity and the steric freedom was found to be most effective for graft polymerization. Grafting with PCL resulted in the production of HAp nanocrystals not only with enhanced colloidal stability but also with excellent dispersion properties in methylene chloride without inter-crystal aggregation, compared with unmodified HAp nanocrystals. Increasing the reactivity of surface hydroxyl groups was a main contributor for effective modification of the HAp surface with PCL, thereby enhancing the interfacial adhesion in HAp/PCL nanocomposites. The nanocomposite of PCL-grafted HAp and PCL exhibited improved mechanical properties compared with that of unmodified HAp and PCL. This was ascribed to the strong adhesion at the interface between HAp and the PCL matrix as well as enhanced dispersibility of PCL-grafted HAp.

The approach described in this study can be extended to a diverse class of inorganic components of which surface properties can be tailored for production of many useful organic−inorganic nanocomposites.

Acknowledgment. This research was supported by a grant (06K1501-01510) from *Center for Nanostructured Materials Technology* under *21st Century Frontier R&D Programs* of the Ministry of Science and Technology, Korea. The authors thank Yong Woo Kim and Geun Hur of KICET for their technical assistance.

CM061139X